

# Charge localization in strongly correlated $\kappa$ -(BEDT-TTF)<sub>2</sub>Cu[N(CN)<sub>2</sub>]I due to inherent disorder

O. Iakutkina,<sup>1,\*</sup> L.N. Majer,<sup>1</sup> T. Biesner,<sup>1</sup> E. Uykur,<sup>1</sup> J.A. Schlueter,<sup>2</sup> and M. Dressel<sup>1</sup>

<sup>1</sup>*1. Physikalisches Institut, Universität Stuttgart, 70569 Stuttgart, Germany*

<sup>2</sup>*Material Science Division, Argonne National Laboratory, Argonne, IL 60439-4831 and National Science Foundation, Alexandria, VA 2223, U.S.A.*

(Dated: November 25, 2021)

In order to understand the physical properties of the series of organic conductors  $\kappa$ -(BEDT-TTF)<sub>2</sub>Cu[N(CN)<sub>2</sub>]X with X = Cl, Br, and I, not only electronic correlations but also the effect of disorder has to be taken into account. While for Cl- and Br-containing salts the influence of both parameters were investigated and a universal phase diagram was proposed, the position of  $\kappa$ -(BEDT-TTF)<sub>2</sub>Cu[N(CN)<sub>2</sub>]I is still not settled. Here we have conducted transport, infrared, and dielectric measurements on single crystals of the title compound to clarify its electronic state at low temperatures. The correlation strength was determined as  $U/W \approx 2.2$ ; thus this salt is placed deeper in an insulating state compare to the two sister compounds. We found that inherent disorder leads to a Coulomb localized insulating state similar to the moderately x-ray-irradiated  $\kappa$ -(BEDT-TTF)<sub>2</sub>Cu[N(CN)<sub>2</sub>]Cl.

## I. INTRODUCTION

The Mott metal-insulator transition is one of the most intriguing phenomena in condensed matter physics [1] that is not completely understood yet. Here the insulating state arises from strong on-site Coulomb repulsion  $U$  with respect to the bandwidth  $W$ . Organic charge-transfer salts are perfectly suited systems for investigating such metal-insulator transition, as they can be easily tuned through the transition both by chemical substitution, or by applying relatively weak hydrostatic pressure. Among them the  $\kappa$ -phase BEDT-TTF compounds have attracted great attention as a bandwidth-controlled Mott system with a variety of exotic ground states [2–5].

The family of isostructural salts  $\kappa$ -(BEDT-TTF)<sub>2</sub>-Cu[N(CN)<sub>2</sub>]X (where BEDT-TTF denotes bis(ethylenedithio)tetrathiafulvalene and X = Cl, Br, I; here abbreviated as  $\kappa$ -Cl,  $\kappa$ -Br, and  $\kappa$ -I, respectively) was discovered in the early 1990s by J.M. Williams and collaborators [6, 7]. By increasing the halogen atom size, the system is expected to go from an insulating to a metallic state. Indeed, the first two salts follow this dependence:  $\kappa$ -Cl is a dimer Mott insulator that becomes superconducting by applying a tiny hydrostatic pressure of only 0.3 kbar ( $T_c = 12.8$  K) [6, 8]. When Cl is replaced by the bigger Br atom,  $\kappa$ -Br shows metallic and even superconducting behavior ( $T_c \approx 11$  K) already at ambient pressure [9]. However, when we go to the even bigger halogen atom - I, the trend does not continue:  $\kappa$ -I is a paramagnetic insulator at ambient pressure and becomes superconducting only under much higher pressures compare to  $\kappa$ -Cl ( $T_c = 8$  K at  $p \approx 1.2$  kbar depending on the quality of crystals) [10–12]. Previous studies inferred that in this case the insulating state arises from superlattice formation in the anion layer [10]. In addition, it was shown that in  $\kappa$ -

I inherent disorder plays an important role and should be considered when describing the low-temperature state [7, 13–15]. For the other two members of the family,  $\kappa$ -Cl and  $\kappa$ -Br, it was recently recognized that disorder – introduced by x-ray irradiation – severely alters the physical properties [16–19]. Therefore, to describe completely all three  $\kappa$ -(BEDT-TTF)<sub>2</sub>Cu[N(CN)<sub>2</sub>]X salts, not only electronic correlations but also disorder has to be considered.

The comprehensive investigation of the physical properties of  $\kappa$ -I by transport measurement, infrared and dielectric spectroscopies, presented here, enables us now to put  $\kappa$ -I in line with the other two members of the  $\kappa$ -(BEDT-TTF)<sub>2</sub>Cu[N(CN)<sub>2</sub>]X family.

## II. MATERIALS AND METHODS

Single crystals of  $\kappa$ -(BEDT-TTF)<sub>2</sub>Cu[N(CN)<sub>2</sub>]I were grown at the Argonne National Laboratory by standard electrochemical oxidation method according to the procedure described in Ref. 12. The crystals have a quasi-two-dimensional structure composed by alternating BEDT-TTF donor layers, separated along the  $b$ -direction by insulating Cu[N(CN)<sub>2</sub>]I<sup>-</sup> sheets, as depicted in Fig. 1. The polymeric anionic zig-zag chains extend along the  $a$ -axis. The BEDT-TTF molecules compose dimers that are tilted with respect to the  $b$ -axis, forming alternating layers in a herring bone fashion. Their inclination in  $a$ -direction results in short contacts between the ethylene end-groups and the anionic chains.

All  $\kappa$ -(BEDT-TTF)<sub>2</sub>Cu[N(CN)<sub>2</sub>]X compounds crystallize in  $Pnma$  space group with  $Z = 4$ , i.e. four dimers per unit cell. While at room temperature the  $c$ -parameter increases with size of the halogen atom, the unit cell shrinks along the  $a$ -axis; hence the area  $a \times c$  needed to pack four donor molecules remains nearly constant for all three compounds [7]. What is the most important here is the aspect ratio  $c/a$ , which reflects the effect of

\* olga.iakutkina@pi1.uni-stuttgart.de

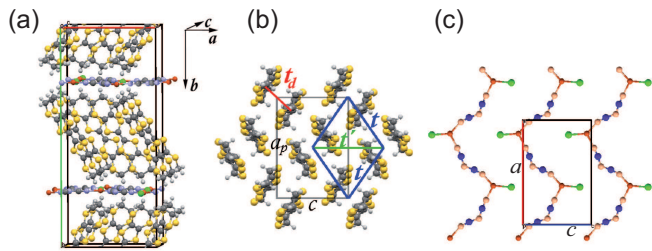


FIG. 1. Crystal structure of  $\kappa$ -(BEDT-TTF) $_2$ Cu[N(CN) $_2$ ]I. The lines mark the unit cell. Carbon, sulfur and hydrogen atoms of the BEDT-TTF molecule are colored in dark gray, yellow and light gray; for the anion chains, iodine, copper, carbon and nitrogen are colored in green, red, blue and orange, respectively. (a) The layers of BEDT-TTF molecules are separated by planes of anions along the  $b$ -direction. The alternating tilting direction of the BEDT-TTF dimers in adjacent layers leads to a doubling of the unit cell. In panels (b) and (c) one cation and anion layer is shown, respectively, where  $a_p$  denotes the projection of the  $a$  axis on the direction perpendicular  $b$  and  $c$  axes. The interdimer transfer integrals are denoted by  $t$  and  $t'$ , and the intradimer transfer integral by  $t_d$ .

chemical pressure on the  $\kappa$ -(BEDT-TTF) $_2$ Cu[N(CN) $_2$ ]X salts [20]. Even though the values of  $c/a$  are very similar in all three salts for  $T = 295$  K, the difference becomes significant at low temperatures, as can be seen from Table I. T. Mori *et al.* showed [20] that for  $c/a$  in the range from 0.640 to 0.675, the correlation strength is reduced upon increasing the axes ratio, in accordance with experimental results for  $\kappa$ -Cl and  $\kappa$ -Br-salts. When the aspect ratio  $c/a$  increases further, the system becomes highly correlated again because the overlap integrals change significantly. This could be exactly the case for  $\kappa$ -(BEDT-TTF) $_2$ Cu[N(CN) $_2$ ]I.

TABLE I. Room-temperature unit-cell data for  $\kappa$ -(BEDT-TTF) $_2$ Cu[N(CN) $_2$ ]X ( $X = \text{Cl, Br, I}$ ) listed together with the axes ratio  $c/a$  for room temperature and for the lowest  $T$  accessible (taken from Ref. 7)

$X =$	Cl	Br	I
$a$ (Å)	12.977	12.942	12.928
$b$ (Å)	29.979	30.016	30.356
$c$ (Å)	8.480	8.539	8.683
$c/a$ ( $T = 295$ K)	0.654	0.660	0.672
$c/a$ ( $T = 127$ K)	0.652	0.659	0.685

The in-plane resistivity along the  $c$ -axis was measured by dc two-point method as a function of temperature. Optical spectroscopy was performed in a broad frequency range at different temperatures utilizing two Fourier transform infrared spectrometers. For covering the high-frequency range (above 600  $\text{cm}^{-1}$ ) a Bruker Vertex 80v spectrometer with an attached Hyperion IR microscope was used, while for the low-frequency range

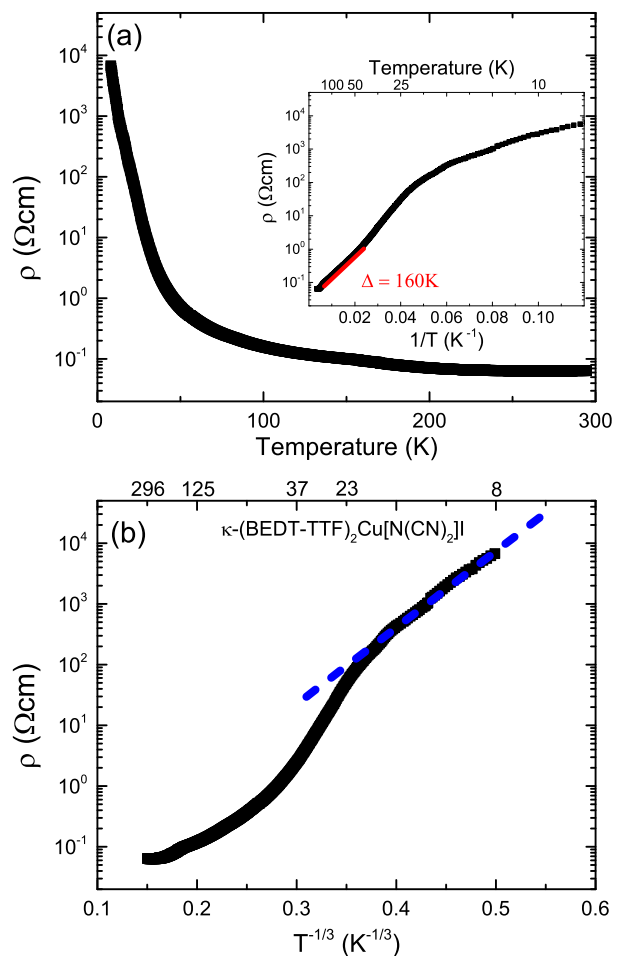


FIG. 2. Temperature dependence of the dc resistivity of  $\kappa$ -(BEDT-TTF) $_2$ Cu[N(CN) $_2$ ]I measured in-plane along the  $c$ -direction. (a) The log-lin representation visualizes the pronounced insulating behavior at low temperatures. From the Arrhenius plot in the inset a thermally activated transport can be identified between 50 and 100 K, where the resistivity follows the red line corresponding to a gap  $\Delta = 160$  K. (b) When plotting the resistivity as a function of  $T^{-1/3}$ ,  $\rho(T)$  can be fitted by the dashed blue line representing two-dimensional variable-range-hopping.

(70-700  $\text{cm}^{-1}$ ) reflectance measurements were performed with a Bruker IFS113v spectrometer applying an *in-situ* freshly evaporated gold overcoating technique. From the reflectivity spectra, the optical conductivity was calculated employing Kramers-Kronig analysis with constant extrapolation for low-frequency range, and standard  $\omega^{-4}$  decay for high frequencies. The temperature dependence of the complex dielectric function  $\hat{\epsilon} = \epsilon' + i\epsilon''$  was measured with the help of an Agilent A4294 impedance analyzer in the frequency range from 100 Hz to 10 MHz along the  $c$ -axis. Using a home-made sample holder enables us to conduct reliable measurements from 5-10 kHz to 5-10 MHz, where the limits depend on the sample resistivity.

### III. RESULTS

#### A. Transport properties

Fig. 2(a) displays the dc resistivity  $\rho(T)$  of  $\kappa$ -(BEDT-TTF)<sub>2</sub>Cu[N(CN)<sub>2</sub>]I recorded along the  $c$ -axis as a function of the temperature. The crystal exhibits a metallic behavior at high  $T$  and becomes insulating below approximately 100 K. A transformation to an insulating state happens in the intermediate range between 230 and 100 K, most likely due to a superstructure formation, which doubles the unit cell in the  $c$ -direction [10]. Interestingly, a similar formation of a  $c^*/2$  superlattice was observed in  $\kappa$ -Br below 200 K while it has not been reported in  $\kappa$ -Cl [21, 22]. Tanatar *et al.* suggested that the real gap in  $\kappa$ -(BEDT-TTF)<sub>2</sub>Cu[N(CN)<sub>2</sub>]I starts opening only below 100 K due to short-range ordering with a wave vector close to  $c^*/3$ , where the resistivity starts to follow thermally activated behavior [10].

The inset of Fig. 2 visualizes the resistivity in an Arrhenius plot illustrating the thermally activated behavior of  $\rho(T)$  between 100 and 50 K; it starts to deviate from the straight line at low temperatures. Despite the limited range, we can extract an energy gap  $\Delta \approx 160$  K that is in accord with previous studies [6, 10, 15]. Below  $T = 25$  K the resistivity is significantly reduced compared to a thermally activated behavior. For systems with inherent disorder, electronic transport can take place via hopping between neighboring sites; in this case the temperature dependence of the resistivity follows the variable-range-hopping (VRH) model, described by

$$\rho(T) \propto \exp\left\{\frac{T_0}{T}\right\}^{1/(1+d)}, \quad (1)$$

where  $d = 2$  for two-dimensional systems. In Fig. 2(b) the dc resistivity is plotted logarithmically versus  $T^{-1/3}$ , and indeed it is clearly seen that the plot is linear at low temperatures ( $T < 25$  K). This supports the idea of disorder important in  $\kappa$ -I at low temperatures; it is in accord with previous findings [10, 13]. However, the temperature where the inhomogeneous electronic state appears is slightly lower than was reported previously (40 K). This can be explained by the different quality of crystals.

#### B. Optical spectroscopy

In Figs. 3 and 4 the reflectivity and the resulting optical conductivity spectra of  $\kappa$ -(BEDT-TTF)<sub>2</sub>Cu[N(CN)<sub>2</sub>]I are plotted for different temperatures; the light is polarized along the two in-plane directions, i.e.  $E \parallel a$  and  $E \parallel c$ . For  $E \parallel c$  the infrared spectra are dominated by the large absorption peaks centered around 2200  $\text{cm}^{-1}$  and 3200  $\text{cm}^{-1}$ . In the perpendicular direction,  $E \parallel a$ , both transitions coincide in energy, resulting in a single

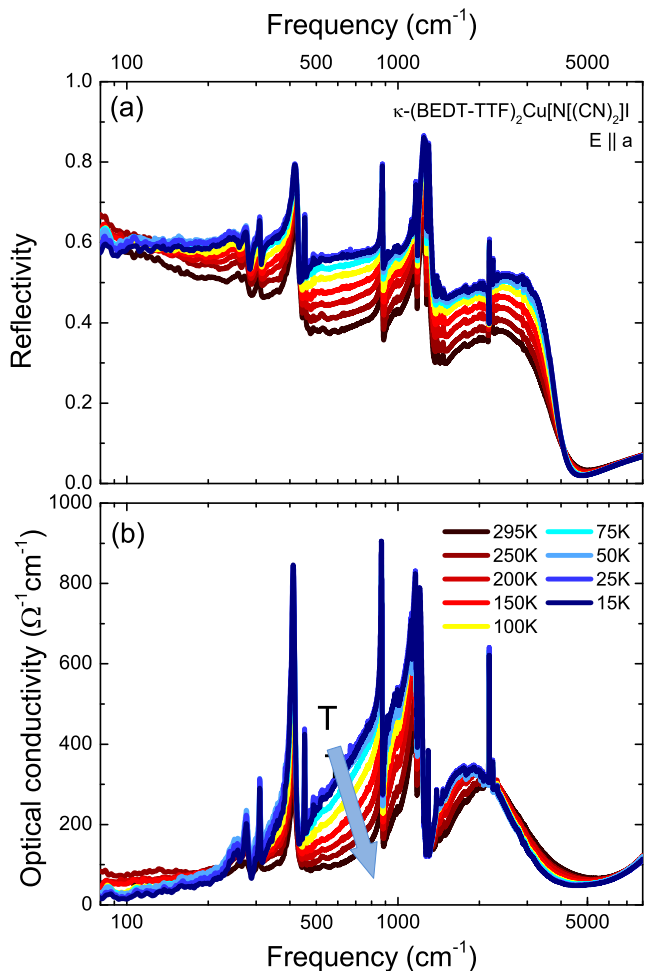


FIG. 3. (a) Optical reflectivity and (b) conductivity spectra of  $\kappa$ -(BEDT-TTF)<sub>2</sub>Cu[N(CN)<sub>2</sub>]I for  $E \parallel a$  polarization (the most conducting axis) recorded between room temperature and  $T = 15$  K.

feature. These bands correspond to intraband transitions between the lower and upper Mott-Hubbard bands and interband between the dimer bands, respectively and are typical for the  $\kappa$ -type phase of the BEDT-TTF salts [3, 23].

In addition to the electronic features, there are strong vibrational signatures at 450, 850 and 1200  $\text{cm}^{-1}$ . These molecular vibrations are assigned to  $\nu_{10}(a_g)$ ,  $\nu_{49}(b_{2u})$  and  $\nu_3(a_g)$  modes of the BEDT-TTF molecules, respectively [24–26]. The two totally symmetric stretching modes can be observed by infrared spectroscopy due to electron-molecular vibration (emv) coupling. In addition, several peaks with smaller intensities are present in conductivity spectra, which are assigned in the Appendix A; we also refer to comprehensive vibrational studies by Eldridge and others [26–28].

At ambient condition,  $\kappa$ -I is a correlated metal, with relatively low reflectivity that continuously drops with frequency; hence the corresponding optical conductivity is rather small. Upon cooling, the crystal becomes in-

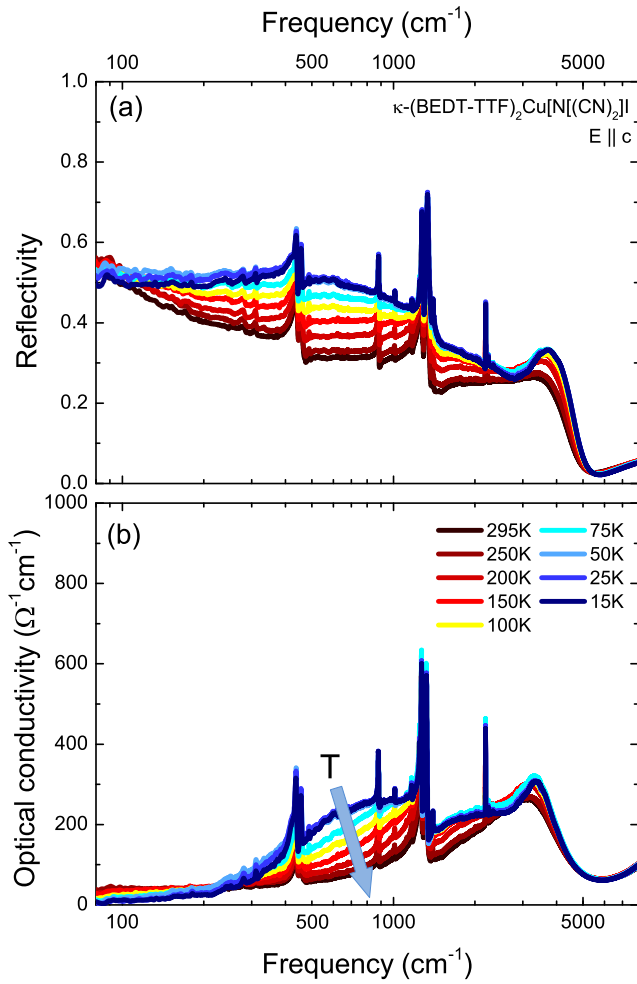


FIG. 4. (a) In-plane reflectivity and (b) optical conductivity of  $\kappa$ -(BEDT-TTF) $_2$ Cu[N(CN) $_2$ ]I measured with  $E \parallel c$ -axis for temperatures between  $T = 295$  and 15 K.

insulating with a frequency-independent reflectivity in the far-infrared range; the Mott gap opens. Reducing the temperature further, a pronounced in-gap absorption in the far-infrared region occurs. The same was observed in the irradiated  $\kappa$ -Cl salt, where the introduction of disorder in the anion layer by x-ray radiation leads to a filling of the Mott gap: the Mott insulating state is transformed to a localization insulating state [16, 17]. The in-gap absorption is more prominent along the  $c$ -direction where electronic properties are stronger affected by the superstructure formation in the anion layers [10], therefore in the discussion we will focus on infrared spectra for the polarization  $E \parallel c$ .

In addition, to make a full comparison of all three  $\kappa$ -(BEDT-TTF) $_2$ Cu[N(CN) $_2$ ]X ( $X = \text{Cl}, \text{Br}, \text{I}$ ) salts, the in-plane reflectivity of  $\kappa$ -Br was measured for  $E \parallel (a, c)$  at  $T = 20$  K, and the optical conductivity was subsequently calculated via Kramers-Kronig transformation. The results will be discussed in Sec. IV.

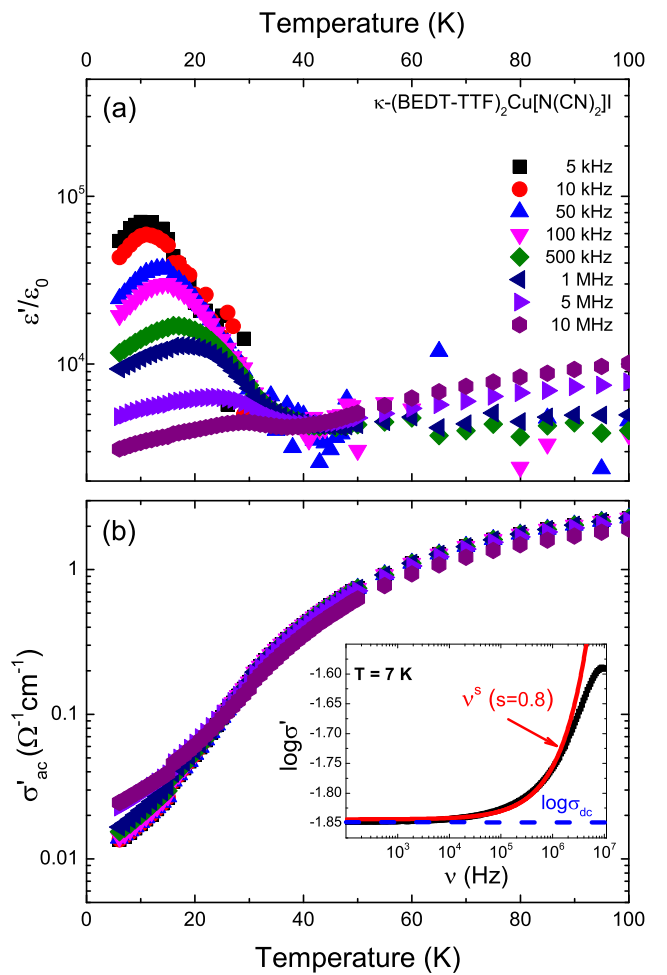


FIG. 5. Temperature dependence of (a) the real part of dielectric constant  $\epsilon'(\omega)/\epsilon_0$  and (b) the real part of the ac conductivity  $\sigma'(\omega)$  of  $\kappa$ -(BEDT-TTF) $_2$ Cu[N(CN) $_2$ ]I for  $E \parallel c$ -axis measured at different frequencies  $\nu$  as indicated. In the insert, the frequency dependence of the low-temperature conductivity  $\sigma'(\omega)$  is shown, where the red line corresponds to a variable-range-hopping fit with the critical exponent  $s = 0.8$  and the offset is equal to the dc contribution  $\sigma_{dc}$ .

### C. Dielectric spectroscopy

The temperature dependence of the dielectric constant is plotted in Fig. 5(a) for various frequencies as indicated. As data for 5 and 10 kHz are quite noisy above 30 K and not displayed. A relaxor-like anomaly is observed below approximately 40 K with the maximum around 10 K in the static limit; the peak in  $\epsilon'(T)$  shifts to higher temperatures as the frequency increases. The ac conductivity  $\sigma' = \omega\epsilon''/4\pi$  also exhibits a frequency dependence that becomes significant below 20 to 25 K as displayed in Fig. 5(b). This relaxational behavior is widely observed in disordered systems such as glass-forming liquids, spin-/cluster glasses, and relaxor ferroelectrics.

In electronic conductors, sufficient disorder can prevent coherent metallic transport and localize charge car-



riers; nevertheless charge transport can take place via hopping between discrete sites. Mott's VRH model gives a theoretical treatment of hopping transport; in Sec. III A it was already successfully applied to describe the temperature-dependent dc conductivity. For the frequency-dependence of the real part of the complex  $\hat{\sigma}(\omega)$ , hopping conduction results in a power law with an exponent  $s < 1$ , according to [29, 30]:

$$\sigma' = \sigma_{dc} + \sigma_0 \nu^s, \quad (2)$$

where  $\sigma_{dc}$  denotes the dc conductivity,  $\sigma_0$  is a prefactor, and  $\nu = \omega/2\pi$  is the applied frequency. From the VRH model  $s \approx 0.8$  is expected [31–33]. Indeed, as it can be seen from the inset of Fig. 5(b),  $\sigma'(\nu)$  can be well described by Eq. (2) with  $s \approx 0.8$  for frequencies below 1 MHz; the deviation at high frequencies may be caused by a weak dependence of  $s$  on frequency. It is interesting to compare these findings with the quantum spin liquid candidates  $\kappa$ -(BEDT-TTF)<sub>2</sub>Cu<sub>2</sub>(CN)<sub>3</sub> and  $\kappa$ -(BEDT-TTF)<sub>2</sub>Ag<sub>2</sub>(CN)<sub>3</sub>, where exponents  $s \approx 0.8 - 1.2$  were reported at low temperatures [34, 35].

## IV. DISCUSSION

### A. Electronic correlations

For the family of  $\kappa$ -(BEDT-TTF)<sub>2</sub>Cu[N(CN)<sub>2</sub>]<sub>2</sub>X ( $X = \text{Cl, Br, I}$ ) both, electronic correlations and disorder are extremely important for understanding the electronic properties; the former one can lead to the Mott metal-insulator transition, the latter one may result in Anderson localization. Sasaki *et al.* previously showed [16, 17] that increasing disorder by successive x-ray irradiation does not affect the fundamental electronic parameters such as on-site Coulomb repulsion  $U$  and bandwidth  $W$ . Since the correlation strength  $U/W$  remains basically unaffected, for all three compounds it can be determined from pristine crystals.

A fit of the optical conductivity by the Drude-Lorentz model has previously [24, 36] been established as a reliable method to determine  $U/W$ . Following this approach we can separate the contributions of conduction electrons, interband transitions, and vibrational features. For comparison, the low-temperature optical conductivity of all three salts are displayed in Fig. 6(a). All data were recorded within the highly conducting ( $a, c$ ) plane, for  $\kappa$ -I and  $\kappa$ -Cl the polarization  $E \parallel c$  is specified. While the Br-compound is a metal with a prominent Drude-like contribution,  $\kappa$ -Cl is insulating with the Mott gap below approximately 1000 cm<sup>-1</sup>.  $\kappa$ -I is an insulator, too, but some pronounced in-gap absorption is present for frequencies below 1000 cm<sup>-1</sup>. For the title compound, inherent disorder leads to a localized insulating state. In general, Mott insulators exhibit a clear cut gap with no density of states at the Fermi level; however, here a finite density of states extends close to  $E_F$  [16]. We should

TABLE II. Electronic parameter of the Hubbard model extracted from fits of the low-temperature optical conductivity spectra in Fig. 6. The mid-infrared peak corresponds to the Coulomb repulsion  $U$ . The electronic bandwidth  $W$  is determined by half of the full width of the absorption band. From these experimental values we calculate the correlation strength  $U/W$  of  $\kappa$ -(BEDT-TTF)<sub>2</sub>Cu[N(CN)<sub>2</sub>]<sub>2</sub>X.

$X =$	Cl	Br	I
$U$ (meV)	289	264	294
$W$ (meV)	161	152	132
$U/W$	1.78	1.40	2.20

recall that the compound is a clear-cut insulator as far as the dc conductivity is concerned, displayed in Fig. 2.

On the first glance, a similar observation was reported for  $\kappa$ -(BEDT-TTF)<sub>2</sub>Cu<sub>2</sub>(CN)<sub>3</sub> [37–39], where a rising in-gap absorption upon cooling could finally be explained by entering the phase-coexistence regime linked to the first-order nature of the Mott transition. The enhanced conductivity corresponds to an enormous peak in the dielectric permittivity due to the percolative nature of the metal-insulator transition [40, 41]. A closer look, however, reveals distinct differences in the spectral and temperature behavior observed in  $\kappa$ -I. Hence, we conclude fundamentally different reasons for the appearance of excess absorption in these Mott insulators.

An enhancement of the conductivity was also reported for  $\kappa$ -Cl after x-ray irradiation [17]. To clarify this point, we compare the low-temperature optical conductivity of the three sibling compounds in Fig. 6(a). The panels (b)–(d) display  $\sigma'(\omega)$  for  $\kappa$ -I at  $T = 15$  K,  $\kappa$ -Cl at  $T = 15$  K, and  $\kappa$ -Br at  $T = 20$  K with separate contributions and the overall fits according to the Drude-Lorentz model. For all three compounds, two Lorentzians and a couple Fano modes (not shown in the plots) are needed to obtain a satisfactory fit in the mid-infrared spectral range. These contributions correspond to intraband transitions, i.e. the transitions within the conduction band split into the lower and upper Hubbard bands ( $L_{\text{Hubbard}}$ ); and interband transitions between the dimer bands (intradimer charge transfer,  $L_{\text{dimer}}$ ) [23]. Fano contributions describe the vibrational modes, which are activated due to emv coupling [3, 24]. In addition, a Drude peak was added in the case of  $\kappa$ -Br to account for the contribution of the conduction electrons, and one extra Lorentzian term for  $\kappa$ -I ( $L_{\text{in-gap}}$ ), which is ascribed to the realization of localized insulating state with a partially filled gap [17].

Most important, from the peak position of  $L_{\text{Hubbard}}$  we can extract the Coulomb repulsion, while the half-width corresponds to the bandwidth. The values for effective correlation strength  $U/W$  obtained from our fits of the optical data  $\sigma'(\omega)$  [42] are listed in Tab. II. For  $\kappa$ -Cl and  $\kappa$ -Br the values extracted from the fits of our spectra are higher than those obtained from *ab-initio* density functional theory (DFT) and extended Hückel calculations [43]. We explain this by the sizable renormalization of

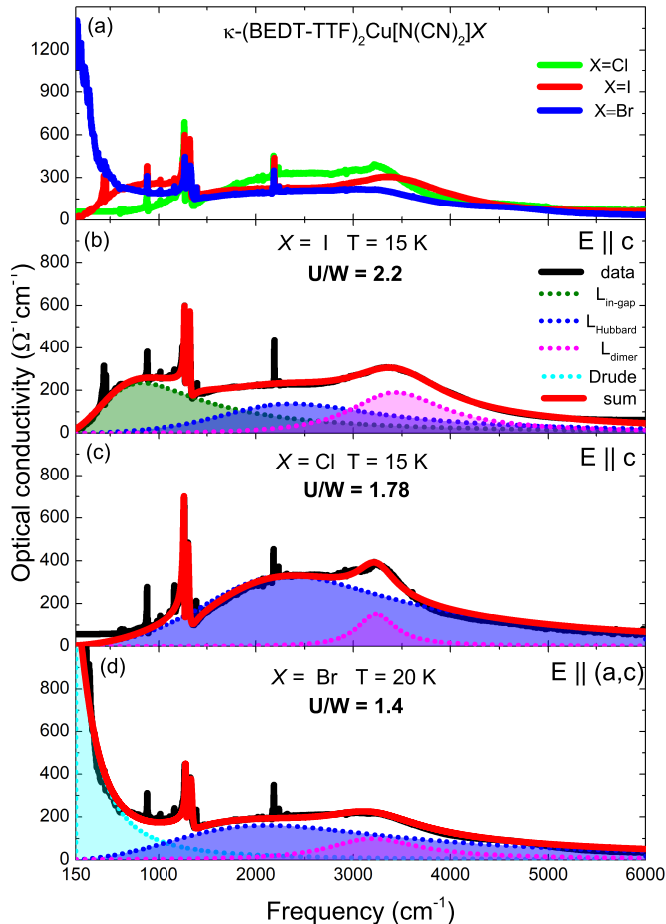


FIG. 6. (a) Frequency dependence of the optical conductivity of three  $\kappa$ -(BEDT-TTF) $_2$ Cu[N(CN) $_2$ ]X salts (X=I, Cl, Br) at the lowest accessible temperatures shown on one graph for comparison. (b) Spectrum of  $\kappa$ -(BEDT-TTF) $_2$ Cu[N(CN) $_2$ ]I at  $T = 15$  K and with  $E \parallel c$ . (c) Spectrum of  $\kappa$ -(BEDT-TTF) $_2$ Cu[N(CN) $_2$ ]Cl at  $T = 15$  K and with  $E \parallel c$ , the data are taken from Ref. 42. (d) Spectrum of  $\kappa$ -(BEDT-TTF) $_2$ Cu[N(CN) $_2$ ]Br at  $T = 20$  K and with  $E \parallel (a, c)$ -plane. All spectra were fitted according to the Drude-Lorentz model with indication of different contributions. The red lines correspond to the sum.

the bandwidth due to electronic correlations; in general the experimentally obtained values are larger than the ones calculated by DFT. The decrease of the correlation strength  $U/W$  when going from  $\kappa$ -Cl to  $\kappa$ -Br corresponds to the common picture of a Mott insulator, on the one hand, and a Fermi liquid on the other hand that becomes even superconducting at low temperatures [3, 5, 39]; by applying a small amount of pressure enhances the bandwidth sufficiently to cross the insulator-metal transition. This picture is confirmed by calculations, too. Along these lines, for  $\kappa$ -I one expects metallic behavior, too, because the size of the anion is bigger. However, the correlation strength obtained from the optical spectrum

is significantly higher. Hence, we have to place the compound deep into the insulating side of the phase diagram, even beyond the Cl-salt. Our findings are in accordance with larger dc resistivity and previous studies [10, 13].

## B. Disorder

The electronic properties of these molecular conductors are not solely determined by correlation strength; also disorder has an important influence. In a series of papers, Sasaki and collaborators showed that x-ray irradiation of  $\kappa$ -Cl and  $\kappa$ -Br mainly affects the heavy Cu atoms introducing disorder in the anion layers [16, 19, 44]. This can be monitored by infrared studies because the vibration modes related to the dicyanamide groups coordinated by the Cu atoms decrease in intensity upon irradiation. The defects created in the anions layers cause a random potential modulation that also affects BEDT-TTF layers.

In the present case of  $\kappa$ -(BEDT-TTF) $_2$ Cu[N(CN) $_2$ ]I, the crystals are of highest quality, pristine and not irradiated; hence the source of disorder is distinctively different. Let us consider the interaction between the anion chains and the BEDT-TTF dimers: It is well known that the terminal ethylene groups are disordered between eclipsed (tilted in the same direction) and staggered conformations (tilted in opposite directions) at room temperature in all three salts,  $\kappa$ -Cl, Br, and I. Importantly, however, is the different behavior observed upon cooling. Pouget *et al.* pointed out [45] that it strongly depends on the donor $\cdots$ donor and donor $\cdots$ anion interactions whether the BEDT-TTF molecules adopt eclipsed or staggered conformations. When looking at the first two salts –  $\kappa$ -Cl and  $\kappa$ -Br – both conformations of the ethylene end-groups are present at room temperature, with a tendency towards the eclipsed conformation (83% for  $\kappa$ -Cl and  $67 \pm 2\%$  for  $\kappa$ -Br) [46, 47]. With lowering the temperature, the eclipsed conformation strongly dominates: for  $\kappa$ -Cl, the end-groups are completely eclipsed below 150 K; while for  $\kappa$ -Br, 97% of the BEDT-TTF molecules possess ethylene groups in the eclipsed conformation. In other words, the CH $_2$  groups are basically ordered in eclipsed configuration at low temperatures and only 3% of the ethylene groups are tilted in opposite directions (staggered conformation). The stabilization of the eclipsed conformation in  $\kappa$ -Cl and  $\kappa$ -Br results from inter-dimer interactions, which dominate over intra-dimer and donor $\cdots$ anion interactions. For the former salt the CH $\cdots$ HC contacts are more strained in the staggered conformation than in case of  $\kappa$ -Br, and they become even shorter upon cooling. Therefore no staggered conformation remains in  $\kappa$ -Cl at low temperatures due to destabilizing repulsive interactions. For  $\kappa$ -Br these interactions are weaker, and some of the end-groups are still staggered at the lowest temperature [45].

In contrast to  $\kappa$ -Cl and  $\kappa$ -Br, the behavior is rather different for  $\kappa$ -I because the terminal ethylene groups stay disordered even at low temperature (70% in eclipsed

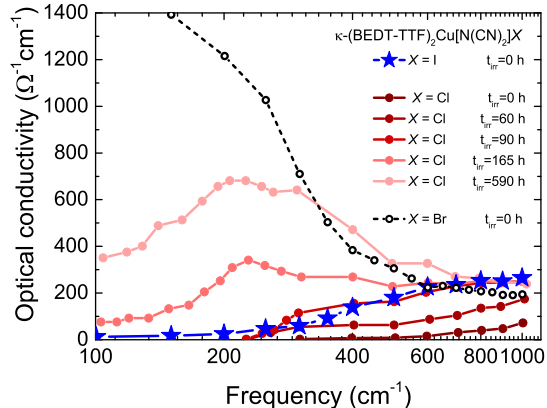


FIG. 7. Values of optical conductivity of  $\kappa$ -(BEDT-TTF) $_2$ Cu[N(CN) $_2$ ]X ( $X = \text{Cl, I, Br}$ ) at different frequencies with different irradiation time ( $t_{\text{irr}}$ ) at the lowest temperature ( $X = \text{Cl}$  data are taken from Ref. [17]).

and 30% in staggered conformations). This behavior is mainly governed by donor $\cdots$ donor interactions: while the eclipsed arrangement leads to strongly strained CH $\cdots$ S contacts, the staggered one results in strongly strained CH $\cdots$ HC contacts. In order to reduce the steric strain in the lattice, the ethylene groups remain disordered even at low temperatures [7]. This disorder causes a random potential that affects the conducting-BEDT-TTF layers in  $\kappa$ -I. It also prevents superconductivity in  $\kappa$ -I at ambient pressure, very similar to the findings in  $\beta$ -(BEDT-TTF) $_2$ I $_3$  [7, 48–50]. It is interesting to note that the donor $\cdots$ anion contacts are shorter in  $\kappa$ -I compare to the Cl and Br-analogues [7].

Although the origin of disorder is different in pristine  $\kappa$ -I with respect to irradiated  $\kappa$ -Cl and  $\kappa$ -Br, in all cases randomness leads to Anderson localization and incoherent transport. To quantify the effect of disorder, let us compare the optical spectra. They provide an integral and energy-resolved property that is very sensitive to the amount of disorder introduced by x-ray irradiation and it can be quantified by the total time of irradiation [16, 17, 19]. It was shown for the insulator  $\kappa$ -Cl that upon increasing the irradiation time there is a significant change of optical conductivity: the spectral weight shifts from the mid-infrared to the far-infrared. As a result, the well-developed Mott-Hubbard gap gradually closes and fills up, indicating the localized insulating state [17]. When we now compare the low-frequency optical conductivity ( $\nu < 1000 \text{ cm}^{-1}$ ) for  $\kappa$ -I with successively irradiated  $\kappa$ -Cl salts, we can quantify the inherent amount of disorder.

To that end, the low-temperature optical conductivity of  $\kappa$ -I is plotted in Fig. 7 in comparison with the spectra of  $\kappa$ -Cl after being irradiated for different amounts of time as indicated. With increasing disorder the gap in  $\kappa$ -Cl closes gradually; at around 90 hours of irradiation, the optical behavior almost coincides with the spectra

of  $\kappa$ -I. We conclude, that in  $\kappa$ -I crystals – even without irradiation – inherent disorder is present, strongly affecting the electronic properties. We trace this effect back to disordered ethylene end-groups of the BEDT-TTF donor molecules. At elevated temperature, for all three salts,  $\kappa$ -Cl,  $\kappa$ -Br and  $\kappa$ -I, dynamical disorder in the terminal ethylene groups dominates with a mixture of the two possible conformations – staggered and eclipsed. Upon cooling the motion of the  $-\text{CH}_2$  groups freezes out, and they become ordered in the first two compounds with preferred eclipsed conformation. In the I-salt, however, the ethylene groups remain disordered with both eclipsed and staggered conformations statistically distributed [7, 13]. This random potential causes a partial localization of charge seen in the optical spectra.

Our final results are in line with recent investigations of  $\kappa$ -(BEDT-TTF) $_2$ Cu[N(CN) $_2$ ]I by NMR spectroscopy where an abrupt line broadening below  $T = 40 \text{ K}$  indicated an electronic inhomogeneity accompanied by antiferromagnetic fluctuations [13]. Angular dependent studies by electron spin resonance spectroscopy also reveal the intrinsic disorder in the spin behavior of  $\kappa$ -I [15]. The transient polarization anisotropy observed by pump probe spectroscopy polarized along the  $c$ -axis might also be related to the disorder in the terminal ethylene groups affecting the electronic properties [14].

### C. Phase diagram

For summarizing our findings, we propose a schematic phase diagram for  $\kappa$ -(BEDT-TTF) $_2$ Cu[N(CN) $_2$ ]X ( $X = \text{Cl, Br, I}$ ) salts in Fig. 8 that presents the temperature-dependent phases as a function of correlation strength ( $U/W$ ) and randomness ( $t_{\text{irr}}$ ). The data from our optical studies are complemented with previous reports [16], in order to place  $\kappa$ -I together with the other members of the family; this way we could determine the exact positions of  $\kappa$ -Cl, Br, and I on the  $U/W$  axis.

In the absence of artificial disorder,  $\kappa$ -Br and Cl are placed close to the Mott transition: on the metallic (superconducting) and Mott insulating side, respectively. Introducing disorder in  $\kappa$ -Br (the plane indicated by the dashed pink line), firstly the superconducting transition temperature decrease. At some critical value of disorder, the system enters the localized insulating state. The Mott insulator  $\kappa$ -Cl, on the other hand, is transformed to a localized insulator only after 60 h of irradiation, as evidenced by the appearance of an in-gap absorption peak in the optical spectra [17]. In the case of  $\kappa$ -I, the presence of inherent disorder at low temperature places the compound in the Anderson-type localization insulator state even without externally introduced disorder. Applying hydrostatic pressure (the plane indicated by the green dashed line in Fig. 8) tunes  $\kappa$ -I through the insulator-to-metal transition, with the superconducting state indicated by the green area [51].

Just to make it clear, this sketch is gross simplified

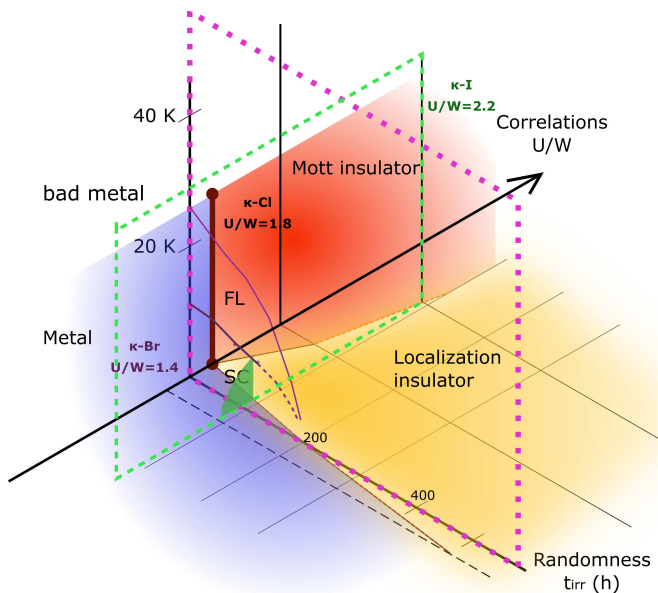


FIG. 8. Schematic phase diagram of  $\kappa$ -(BEDT-TTF) $_2$ Cu[N(CN) $_2$ ]X ( $X = \text{Br, Cl, I}$ ) for temperature, effective correlation strength ( $U/W$ ), and randomness ( $t_{\text{irr}}$ ). The thick brown line indicates the border between metallic and insulating states terminated by the critical end point. The plane indicated by the dashed pink line shows how the electronic state of  $\kappa$ -(BEDT-TTF) $_2$ Cu[N(CN) $_2$ ]Br is modified when disorder is introduced; the superconducting (SC) and Fermi-liquid (FL) states are also marked [16]. The position of  $\kappa$ -(BEDT-TTF) $_2$ Cu[N(CN) $_2$ ]Cl is shown by the vertical black line at  $t_{\text{irr}} = 0$  h. The plane surrounded by the dashed green line corresponds to the change of the  $\kappa$ -(BEDT-TTF) $_2$ Cu[N(CN) $_2$ ]I ground state by applying hydrostatic pressure, the superconducting phase is represented by the green area [51]. The solid black line here corresponds to  $\kappa$ -(BEDT-TTF) $_2$ Cu[N(CN) $_2$ ]I at ambient pressure.

with only borders between metallic (superconducting), Mott insulating, and localized insulating phases shown. As the Mott transition is the first-order transition, a phase-coexistence region is expected at the border of metal and insulator in the absence of disorder [52]. For a high degree of randomness a Griffiths-like phase was suggested recently [53–55]. For more detailed exploration of these states, optical and dielectric investigations under the pressure are highly desirable.

## V. CONCLUSIONS

Our comprehensive investigations of the charge transport, dielectric response and infrared behavior of  $\kappa$ -(BEDT-TTF) $_2$ Cu[N(CN) $_2$ ]I yield valuable information on its electronic properties that allows us to locate  $\kappa$ -I in a global phase diagram with respect to the other members of the  $\kappa$ -(BEDT-TTF) $_2$ Cu[N(CN) $_2$ ]X family. When going from  $\kappa$ -Br to  $\kappa$ -Cl, and finally to  $\kappa$ -I, the electronic correlations strength increases monotonously,

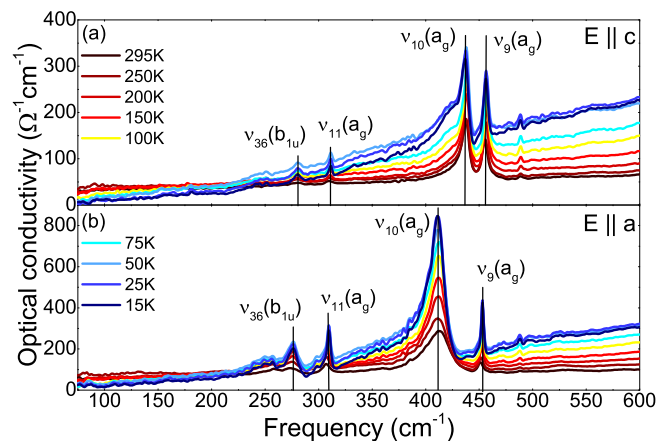


FIG. 9. In-plane optical conductivity of  $\kappa$ -I in far-infrared spectral range measured for different temperatures with the polarization (a)  $E \parallel c$  and (b)  $E \parallel a$ .

and reaches  $U/W = 2.2$  for the title compound; in other words,  $\kappa$ -I is situated deeper in the insulating regime than previously expected. This contrasts suggestions based on the atomic radius. However,  $\kappa$ -I does not represent a clear-cut Mott insulator; even below  $T \approx 25$  K there remains a finite density of states near the Fermi level. By comparing the optical spectra we identify  $\kappa$ -I as a Coulomb localized insulator, similar to  $\kappa$ -Cl when severely disordered by x-ray irradiation for a period of  $t_{\text{irr}} = 90$  h. The  $\kappa$ -(BEDT-TTF) $_2$ Cu[N(CN) $_2$ ]X compounds appear now in a new light, as our findings indicate that not only electronic interactions determine the physical behavior but also the role of disorder is crucial for the understanding of these compounds. These conclusions are more general and might hold for most correlated electron systems.

## ACKNOWLEDGMENTS

We thank Gabriele Untereiner for the indispensable technical assistance. The work was supported by the Deutsche Forschungsgemeinschaft (DFG) via DR228/39-3 and DR228/52-1.

## Appendix A: Vibrational modes

Fig. 9 shows the optical conductivity of  $\kappa$ -I for both in-plane axes recorded in the far-infrared range at different temperatures. The strong vibrational modes at 280, 310, 440 and 460  $\text{cm}^{-1}$  for  $E \parallel c$ , and at 275, 309, 409 and 450  $\text{cm}^{-1}$  for  $E \parallel a$  are assigned to the  $\nu_{36}(b_{1u})$ ,  $\nu_{11}(a_g)$ ,  $\nu_{10}(a_g)$  and  $\nu_9(a_g)$  intra-molecular vibrations of BEDT-TTF [24, 26–28].

In the mid-infrared spectral range, for both polarizations the most dominant features are the totally-symmetric  $\nu_3(a_g)$  vibrations of the C=C double bonds ac-



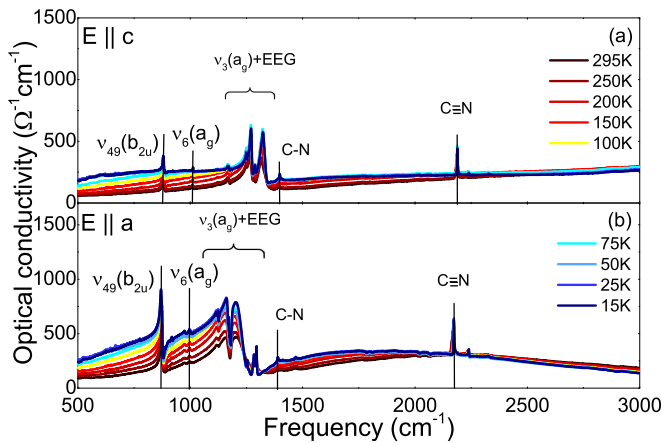


FIG. 10. Mit-infrared spectra of  $\kappa$ -I along (a) the  $E \parallel c$  and (b) the  $E \parallel a$  polarization for different temperatures.

tivated via emv coupling (Fig. 10). It appears as a broad resonance between 1250 and 1350  $\text{cm}^{-1}$  for  $E \parallel c$ , and between 1100 and 1250  $\text{cm}^{-1}$  for  $E \parallel a$ . Vibrations of the ethylene endgroups result in four  $\nu_5(a_g)$  peaks observed at the lower edge of the main resonance for  $E \parallel a$ , and antiresonant dips in the  $E \parallel c$  spectra [26, 27]. Here the  $\nu_3$  mode is shifted to lower frequency compare to  $\kappa$ -(BEDT-TTF) $_2$ Cu[N(CN) $_2$ ]Br in agreement with higher correlation strength in the former one [56]. In addition, the other strong modes in Fig. 10 were assigned to  $\nu_{49}(b_{2u})$ ,  $\nu_6(a_g)$ , and vibrations related to the dicyanamide group of the anion molecule [16, 19, 57].

- [1] N. Mott, *Metal-Insulator Transitions* (Taylor and Francis, London, 1990).
- [2] K. Miyagawa, K. Kanoda, and A. Kawamoto, NMR Studies on Two-Dimensional Molecular Conductors and Superconductors: Mott Transition in  $\kappa$ -(BEDT-TTF) $_2$ X, *Chem. Rev.* **104**, 5635 (2004).
- [3] D. Faltermeier, J. Barz, M. Dumm, M. Dressel, N. Drichko, B. Petrov, V. Semkin, R. Vlasova, C. Mézière, and P. Batail, Bandwidth-controlled Mott transition in  $\kappa$ -(BEDT-TTF) $_2$ Cu[N(CN) $_2$ ]Br $_x$ Cl $_{1-x}$ : Optical studies of localized charge excitations, *Phys. Rev. B* **76**, 165113 (2007); M. Dumm, D. Faltermeier, N. Drichko, M. Dressel, C. Mézière, and P. Batail, Bandwidth-controlled Mott transition in  $\kappa$ -(BEDT-TTF) $_2$ Cu[N(CN) $_2$ ]Br $_x$ Cl $_{1-x}$ : Optical studies of correlated carriers, *Phys. Rev. B* **79**, 195106 (2009).
- [4] S. Yasin, M. Dumm, B. Salameh, P. Batail, C. Mézière, and M. Dressel, Transport studies at the Mott transition of the two-dimensional organic metal  $\kappa$ -(BEDT-TTF) $_2$ Cu[N(CN) $_2$ ]Br $_x$ Cl $_{1-x}$ , *Eur. Phys. J. B* **79**, 383 (2011).
- [5] M. Dressel and S. Tomić, Molecular quantum materials: electronic phases and charge dynamics in two-dimensional organic solids, *Adv. Phys.* **69**, 1 (2020).
- [6] H. Wang, K. Carlson, U. Geiser, A. Kini, A. Schultz, J. Williams, L. Montgomery, W. Kwok, U. Welp, K. Vandervoort, S. Boryschuk, A. Crouch, J. Kammers, D. Watkins, J. Schirber, D. Overmyer, D. Jung, J. Novoa, and M.-H. Whangbo, New  $\kappa$ -phase materials,  $\kappa$ -(ET) $_2$ Cu[N(CN) $_2$ ]X. X=Cl, Br and I. The synthesis, structure and superconductivity above 11 K in the Cl ( $T_c = 12.8$  K, 0.3 kbar) and Br ( $T_c = 11.6$  K) salts, *Synth. Met.* **42**, 1983 (1991).
- [7] U. Geiser, A. J. Schultz, H. H. Wang, D. M. Watkins, D. L. Stupka, J. M. Williams, J. Schirber, D. Overmyer, D. Jung, J. Novoa, and M.-H. Whangbo, Strain index, lattice softness and superconductivity of organic donor-molecule salts: Crystal and electronic structures of three isostructural salts  $\kappa$ -(BEDT-TTF) $_2$ Cu[N(CN) $_2$ ]X (X=Cl, Br, I), *Physica C* **174**, 475 (1991).
- [8] J. M. Williams, A. M. Kini, H. H. Wang, K. D. Carlson, U. Geiser, L. K. Montgomery, G. J. Pyrka, D. M. Watkins, and J. M. Kammers, From semiconductor-semiconductor transition (42 K) to the highest- $T_c$  organic superconductor,  $\kappa$ -(ET) $_2$ Cu[N(CN) $_2$ ]Cl ( $T_c = 12.5$  K), *Inorg. Chem.* **29**, 3272 (1990).
- [9] A. M. Kini, U. Geiser, H. H. Wang, K. D. Carlson, J. M. Williams, W. K. Kwok, K. G. Vandervoort, J. E. Thompson, and D. L. Stupka, A new ambient-pressure organic superconductor,  $\kappa$ -(ET) $_2$ Cu[N(CN) $_2$ ]Br, with the highest transition temperature yet observed (inductive onset  $T_c = 11.6$  K, resistive onset = 12.5 K), *Inorg. Chem.* **29**, 2555 (1990).
- [10] M. A. Tanatar, S. Kagoshima, T. Ishiguro, H. Ito, V. S. Yefanov, V. A. Bondarenko, N. D. Kushch, and E. B. Yagubskii, Electronic transport properties and structural transformations of  $\kappa$ -(BEDT-TTF) $_2$ Cu[N(CN) $_2$ ]I, *Phys. Rev. B* **62**, 15561 (2000).
- [11] N. D. Kushch, M. A. Tanatar, E. B. Yagubskii, and T. Ishiguro, Superconductivity of  $\kappa$ -(BEDT-TTF) $_2$ Cu[N(CN) $_2$ ]I under pressure, *J. Exp. Theor. Phys. Lett.* **73**, 429 (2001).
- [12] N. D. Kushch, M. A. Tanatar, T. Ishiguro, S. Kagoshima, E. B. Yagubskii, V. S. Yefanov, and V. A. Bondarenko, Superconductivity of the  $\kappa$ -(BEDT-TTF) $_2$ Cu[N(CN) $_2$ ]I salt under pressure, *Synth. Met.* **133-134**, 177 (2003).
- [13] T. Kobayashi, A. Suzuta, K. Tsuji, Y. Ihara, and A. Kawamoto, Inhomogeneous electronic state of organic conductor  $\kappa$ -(BEDT-TTF) $_2$ Cu[N(CN) $_2$ ]I studied by  $^{13}\text{C}$  NMR spectroscopy, *Phys. Rev. B* **100**, 195115 (2019).
- [14] S. Tsuchiya, R. Kuwae, T. Kodama, Y. Nakamura, M. Kurihara, T. Yamamoto, T. Naito, and Y. Toda, Electronic Inhomogeneity in Organic Charge Transfer Salt  $\kappa$ -(BEDT-TTF) $_2$ Cu[N(CN) $_2$ ]I Probed by Polarized Femtosecond Spectroscopy, *J. Phys. Soc. of Jpn.* **89**, 064712 (2020).
- [15] L. N. Majer, B. Miksch, O. Iakutkina, T. Kobayashi, A. Kawamoto, and M. Dressel, Interacting electron spins in  $\kappa$ -(BEDT-TTF) $_2$ Cu[N(CN) $_2$ ]I investigated by ESR spectroscopy, *Phys. Rev. B* **102**, 214430 (2020).

- [16] T. Sasaki, Mott-Anderson Transition in Molecular Conductors: Influence of Randomness on Strongly Correlated Electrons in the  $\kappa$ -(BEDT-TTF)<sub>2</sub>X System, *Crystals* **2**, 374 (2012).
- [17] T. Sasaki, N. Yoneyama, Y. Nakamura, N. Kobayashi, Y. Ikemoto, T. Moriwaki, and H. Kimura, Optical Probe of Carrier Doping by X-Ray Irradiation in the Organic Dimer Mott Insulator  $\kappa$ -(BEDT-TTF)<sub>2</sub>Cu[N(CN)<sub>2</sub>]Cl, *Phys. Rev. Lett.* **101**, 206403 (2008).
- [18] K. Sano, T. Sasaki, N. Yoneyama, and N. Kobayashi, Electron Localization near the Mott Transition in the Organic Superconductor  $\kappa$ -(BEDT-TTF)<sub>2</sub>Cu[N(CN)<sub>2</sub>]Br, *Phys. Rev. Lett.* **104**, 217003 (2010).
- [19] T. Sasaki, K. Sano, H. Sugawara, N. Yoneyama, and N. Kobayashi, Influence of randomness on the Mott transition in  $\kappa$ -(BEDT-TTF)<sub>2</sub>X, *phys. stat. sol. (b)* **249**, 947 (2012).
- [20] T. Mori, H. Mori, and S. Tanaka, Structural genealogy of BEDT-TTF-based organic conductors II. inclined molecules:  $\theta$ ,  $\alpha$ , and  $\kappa$  phases, *B. Chem. Soc. Jpn.* **72**, 179 (1999).
- [21] M. Watanabe, Y. Nogami, K. Oshima, H. Ito, T. Ishiguro, and G. Saito, Low temperature superstructure and transfer integrals in  $\kappa$ -(BEDT-TTF)<sub>2</sub>Cu[N(CN)<sub>2</sub>]X: X = Cl, Br, *Synth. Met.* **103**, 1909 (1999).
- [22] Y. Nogami, J. P. Pouget, H. Ito, T. Ishiguro, and G. Saito, Superlattice structural transition in the organic superconductor  $\kappa$ -(BEDT-TTF)<sub>2</sub>Cu[N(CN)<sub>2</sub>]Br, *Solid State Commun.* **89**, 113 (1994).
- [23] J. Ferber, K. Foyevtsova, H. O. Jeschke, and R. Valentí, Unveiling the microscopic nature of correlated organic conductors: The case of  $\kappa$ -(ET)<sub>2</sub>Cu[N(CN)<sub>2</sub>]Br<sub>x</sub>Cl<sub>1-x</sub>, *Phys. Rev. B* **89**, 205106 (2014).
- [24] M. Dressel and N. Drichko, Optical Properties of Two-Dimensional Organic Conductors: Signatures of Charge Ordering and Correlation Effects, *Chem. Rev.* **104**, 5689 (2004).
- [25] A. Girlando, Charge Sensitive Vibrations and Electron-Molecular Vibration Coupling in Bis(ethylenedithio)-tetrathiafulvalene (BEDT-TTF), *J. Phys. Chem. C* **115**, 19371 (2011).
- [26] J. E. Eldridge, Y. Xie, H. H. Wang, J. M. Williams, A. M. Kini, and J. A. Schlueter, Electron-phonon effects in the organic superconductor  $\kappa$ -(BEDT-TTF)<sub>2</sub>Cu[N(CN)<sub>2</sub>]Br, *Spectrochim. Acta A* **52**, 45 (1996).
- [27] J. Eldridge, K. Kornelsen, H. Wang, J. M. Williams, A. Strieby Crouch, and D. Watkins, Infrared optical properties of the 12k organic superconductor  $\kappa$ -(BEDT-TTF)<sub>2</sub>Cu[N(CN)<sub>2</sub>]Br, *Solid State Commun* **79**, 583 (1991).
- [28] J. Eldridge, C. Homes, J. M. Williams, A. Kini, and H. Wang, The assignment of the normal modes of the BEDT-TTF electron-donor molecule using the infrared and Raman spectra of several isotopic analogs, *Spectrochim Acta A* **51**, 947 (1995).
- [29] A. K. Jonscher, *Dielectric Relaxation in Solids* (Chelsea Dielectrics Press, London, 1983).
- [30] A. K. Jonscher, Dielectric relaxation in solids, *J. Phys. D: Appl. Phys.* **32**, R57 (1999).
- [31] S. R. Elliott, A.c. conduction in amorphous chalcogenide and pnictide semiconductors, *Adv. Phys.* **36**, 135 (1987).
- [32] N. F. Mott and A. D. Edward, *Electronic Processes in Non-Crystalline Materials* (Oxford University Press, Oxford, 2012).
- [33] J. C. Dyre and T. B. Schröder, Universality of ac conduction in disordered solids, *Rev. Mod. Phys.* **72**, 873 (2000).
- [34] A. Pustogow, Y. Saito, E. Zhukova, B. Gorshunov, R. Kato, T.-H. Lee, S. Fratini, V. Dobrosavljević, and M. Dressel, Low-Energy Excitations in Quantum Spin Liquids Identified by Optical Spectroscopy, *Phys. Rev. Lett.* **121**, 056402 (2018).
- [35] M. Dressel and A. Pustogow, Electrodynamics of quantum spin liquids, *J. Phys.: Condens. Matter* **30**, 203001 (2018).
- [36] M. Dressel and G. Grüner, *Electrodynamics of Solids* (Cambridge University Press, Cambridge, 2002).
- [37] I. Kézsmárki, Y. Shimizu, G. Mihály, Y. Tokura, K. Kanoda, and G. Saito, Depressed charge gap in the triangular-lattice mott insulator  $\kappa$ -(ET)<sub>2</sub>Cu<sub>2</sub>(CN)<sub>3</sub>, *Phys. Rev. B* **74**, 201101 (2006).
- [38] S. Elsässer, D. Wu, M. Dressel, and J. A. Schlueter, Power-law dependence of the optical conductivity observed in the quantum spin-liquid compound  $\kappa$ -(BEDT-TTF)<sub>2</sub>Cu<sub>2</sub>(CN)<sub>3</sub>, *Phys. Rev. B* **86**, 155150 (2012).
- [39] A. Pustogow, M. Bories, A. Löhle, R. Rösslhuber, E. Zhukova, B. Gorshunov, S. Tomić, J. A. Schlueter, R. Hübner, T. Hiramatsu, Y. Yoshida, G. Saito, R. Kato, T.-H. Lee, V. Dobrosavljević, S. Fratini, and M. Dressel, Quantum spin liquids unveil the genuine Mott state, *Nat. Mater.* **17**, 773 (2018).
- [40] A. Pustogow, R. Rösslhuber, Y. Tan, E. Uykur, A. Böhme, M. Wenzel, Y. Saito, A. Löhle, R. Hübner, A. Kawamoto, J. A. Schlueter, V. Dobrosavljević, and M. Dressel, Low-temperature dielectric anomaly arising from electronic phase separation at the mott insulator-metal transition, *npj Quantum Materials* **6**, 10.1038/s41535-020-00307-0 (2021).
- [41] R. Rösslhuber, A. Pustogow, E. Uykur, A. Böhme, A. Löhle, R. Hübner, J. A. Schlueter, Y. Tan, V. Dobrosavljević, and M. Dressel, Phase coexistence at the first-order mott transition revealed by pressure-dependent dielectric spectroscopy of  $\kappa$ -(BEDT-TTF)<sub>2</sub>Cu<sub>2</sub>(CN)<sub>3</sub>, *Phys. Rev. B* **103**, 125111 (2021).
- [42] K. Sedlmeier, S. Elsässer, D. Neubauer, R. Beyer, D. Wu, T. Ivek, S. Tomić, J. A. Schlueter, and M. Dressel, Absence of charge order in the dimerized  $\kappa$ -phase BEDT-TTF salts, *Phys. Rev. B* **86**, 245103 (2012).
- [43] H. C. Kandpal, I. Opahle, Y.-Z. Zhang, H. O. Jeschke, and R. Valentí, Revision of Model Parameters for  $\kappa$ -Type Charge Transfer Salts: An Ab Initio Study, *Phys. Rev. Lett.* **103**, 067004 (2009).
- [44] N. Yoneyama, T. Sasaki, N. Kobayashi, K. Furukawa, and T. Nakamura, X-ray irradiation effect on magnetic properties of Dimer-Mott insulators:  $\kappa$ -(BEDT-TTF)<sub>2</sub>Cu[N(CN)<sub>2</sub>]Cl and  $\beta'$ -(BEDT-TTF)<sub>2</sub>ICl<sub>2</sub>, *Physica B* **405**, S244 (2010).
- [45] J.-P. Pouget, P. Alemany, and E. Canadell, Donor-anion interactions in quarter-filled low-dimensional organic conductors, *Mater. Horiz.* **5**, 590 (2018).
- [46] T. Hiramatsu, Y. Yoshida, G. Saito, A. Otsuka, H. Yamochi, M. Maesato, Y. Shimizu, H. Ito, and H. Kishida, Quantum spin liquid: design of a quantum spin liquid next to a superconducting state based on a dimer-type ET Mott insulator, *J. Mater. Chem. C* **3**, 1378 (2015).
- [47] A. U. B. Wolter, R. Feyerherm, E. Dudzik, S. Süllow, C. Strack, M. Lang, and D. Schweitzer, Deter-

- mining ethylene group disorder levels in  $\kappa$ -(BEDT-TTF)<sub>2</sub>Cu[N(CN)<sub>2</sub>]Br, *Phys. Rev. B* **75**, 104512 (2007).
- [48] M. H. Whangbo, J. M. Williams, A. J. Schultz, T. J. Emge, and M. A. Beno, Importance of intermolecular Hydrogen···Hydrogen and Hydrogen···anion contacts for the lattice softness, the electron-phonon coupling, and the superconducting transition temperatures,  $T_c$ , of organic conducting salts  $\beta$ -(ET)<sub>2</sub>X ( $X^- = \text{IBr}_2^-, \text{AuI}_2^-, \text{I}_3^-$ ), *J. Am. Chem. Soc.* **109**, 90 (1987).
- [49] S. Ravy, J. P. Pouget, R. Moret, and C. Lenoir, X-ray study of the incommensurate modulation of the organic superconductor  $\beta$ -di[bis(ethylenedithio)tetrathiafulvalene]tri-iodide, *Phys. Rev. B* **37**, 5113 (1988).
- [50] A. J. Schultz, M. A. Beno, H. H. Wang, and J. M. Williams, Neutron-diffraction evidence for ordering in the high- $T_c$  phase of  $\beta$ -di[bis(ethylenedithio)tetrathiafulvalene]triiodide [ $\beta^*$ -(ET)<sub>2</sub>I<sub>3</sub>], *Phys. Rev. B* **33**, 7823 (1986).
- [51] M. A. Tanatar, T. Ishiguro, S. Kagoshima, N. D. Kushch, and E. B. Yagubskii, Pressure-temperature phase diagram of the organic superconductor  $\kappa$ -(BEDT-TTF)<sub>2</sub>Cu[N(CN)<sub>2</sub>]I, *Phys. Rev. B* **65**, 064516 (2002).
- [52] P. Limelette, P. Wzietek, S. Florens, A. Georges, T. A. Costi, C. Pasquier, D. Jérôme, C. Mézière, and P. Batail, Mott transition and transport crossovers in the organic compound  $\kappa$ -(BEDT-TTF)<sub>2</sub>Cu[N(CN)<sub>2</sub>]Cl, *Phys. Rev. Lett.* **91**, 016401 (2003).
- [53] I. F. Mello, L. Squillante, G. O. Gomes, A. C. Seridonio, and M. de Souza, Griffiths-like phase close to the Mott transition, *J. Appl. Phys.* **128**, 225102 (2020).
- [54] E. C. Andrade, E. Miranda, and V. Dobrosavljević, Electronic Griffiths Phase of the  $d = 2$  Mott Transition, *Phys. Rev. Lett.* **102**, 206403 (2009).
- [55] R. Yamamoto, T. Furukawa, K. Miyagawa, T. Sasaki, K. Kanoda, and T. Itou, Electronic Griffiths Phase in Disordered Mott-Transition Systems, *Phys. Rev. Lett.* **124**, 046404 (2020).
- [56] T. Sasaki and N. Yoneyama, Spatial mapping of electronic states in  $\kappa$ -(BEDT-TTF)<sub>2</sub>X using infrared reflectivity, *Sci. Technol. Adv. Mat.* **10**, 024306 (2009).
- [57] B. Jürgens, W. Milius, P. Morys, and W. Schnick, Trimerisierung von Dicyanamid-Ionen  $\text{C}_2\text{N}_3^-$  im Festkörper-Synthesen, Kristallstrukturen und Eigenschaften von  $\text{NaCs}_2(\text{C}_2\text{N}_3)_3$  und  $\text{Na}_3\text{C}_6\text{N}_9 \cdot 3\text{H}_2\text{O}$ , *Z. Anorg. Allg. Chem.* **624**, 91.